Monteseguro, V.; Errandonea, D.; Achary, SN.; Sans-Tresserras, JÁ.; Manjón, F.; Gallego-Parra, S.; Popescu, C. (2019). Structural Characterization of Aurophilic Gold(I) Iodide under High Pressure. Inorganic Chemistry. 58(16):10665-10670. https://doi.org/10.1021/acs.inorgchem.9b00433

Discovery of pressure-induced polymorphic transition and amorphization of aurophilic gold iodide

Virginia Monteseguro,[1] Daniel Errandonea,[1] S. Nagabhusan Achary,[2] Juan A. Sans,[3] F. Javier Manjón,[3] Samuel Gallego-Parra,[3] and Catalin Popescu[4]*

[1]Departamento de Física Aplicada-ICMUV, MALTA Consolider Team, Universitat de Valencia, Edificio de Investigación, c/Dr. Moliner 50, Burjassot, 46100 Valencia, Spain.

[2] Bhabha Atomic Research Center, Chem. Div., Bombay 400085, Maharashtra, India.

[3] Instituto de Diseño para la Fabricación y Producción Automatizada, MALTA Consolider Team, Universitat Politècnica de València, 46022 Valencia, Spain.

[4] CELLS-ALBA Synchrotron Light Facility, 08290 Cerdanyola, Barcelona, Spain.

KEYWORDS: Gold Iodide, Aurophilicity, Barocaloric material, high-pressure

ABSTRACT: The effects of pressure on the crystal structure of aurophilic tetragonal gold iodide have been studied by means of powder x-ray diffraction up to 13.5 GPa. We found evidence of the onset of a structural first-order transition at 1.5 GPa with an associated 5% volume collapse. The low- and high-pressure phases coexist from this pressure up to 3.3 GPa. At 3.8 GPa the phase transformation is completed and the high-pressure polymorph remains stable up to 10.7 GPa. The phase of high-pressure polymorph suggested is a monoclinic crystal structure and it is more densely packed than the layered structure of aurophilic gold iodide, involving the formation of I-I bonds and a three dimensional arrangement. Beyond 10.7 GPa, an irreversible process of

amorphization takes place. We determined the axial and bulk compressibility of both phases of gold iodide. The tetragonal phase is extremely compressible with a bulk modulus of 18.1(8) GPa and its response to pressure is anisotropic. On the other hand, the monoclinic phase shows a smaller compressibility with a bulk modulus 31.8(1.5) GPa. Phase transitions have been discussed from a crystallographic point of view. Our work reveals the shortest pressure-induced Au-Au aurophilic distance, 2.845 Å at 4.9 GPa, in a 3D fully inorganic gold(I) iodide structure.

1. INTRODUCTION

The expansion of high-pressure (HP) research due to the development of diamond-anvil cells and associated characterization techniques has led to many important breakthroughs during the last decade.[1] In particular, high-pressure could radically modify the physical and chemical properties of materials leading frequently to unexpected structural transformations.[2] This has recently driven the discovery of new materials or new phases of known materials with unique properties.[3, 4] Among inorganic compounds a vast majority of HP studies have been focused on nitrides and oxides.[3, 5] In contrast with those inorganic compounds, fewer efforts have been devoted to study the behavior under compression of aurophilic compounds, like gold iodide (AuI).

The most important feature of the AuI is the enticing interaction between closed-shell Au^+ centers. It is the general trend of metal (M) aggregates to reproduce the topology of their metallic fcc-structures. Thus, M-M distances of such aggregates take values close to these observed in their metallic structures.[6] They are clearly shorter than the sum of two van der Waals radii (3.7 Å), in favorable cases as short as 2.7 Å, but generally around 3 Å.[7] This interaction is commonly referred as aurophilic bonding and in general it has a strength between 29 and 46 KJ/mol, similar to that of the hydrogen bonding. Such interaction gives rise to the formation of dimers, oligomers, and

infinite chains.[8, 9] This effect is larger for Au than for copper (Cu) or silver (Ag) due to relativistic effects of the former. The 28% of the binding energy in Au^+ complexes with aurophilic interactions can be attributed to relativistic expansion of the Au-d orbitals.[10] Currently, the similarity in strength between hydrogen bonding and aurophilic interaction has proven to be a convenient tool in the field of polymer and supramolecular chemistry. To date, the study of the aurophilicity under high pressure has been very limited.[11, 12] For this reason, our HP crystallographic study will improve the understanding of the HP behavior of these aurophilic materials, i.e. as the pressure affects to the Au-Au interaction that gives rise to aurophilic bonds within inorganic structures.

On the other hand, the interest on the HP behavior of metal iodides has been recently stimulated by the discovery that pressure-driven structural changes can induce a giant barocaloric effect in silver iodide (AgI). Such an effect is associated with a pressure-driven decrease of the superionic transition temperature.[13] This phenomenon can be extremely useful for developing environmentally friendly cooling devices.[14, 15] Such a breakthrough has shown the need for information of the influence of pressure in the crystal structures of AgI and other noble-metal iodides, like AuI and copper iodide (CuI). In this context, the crystal structure of AgI has been studied up to nearly 10 GPa and up to four different polymorphs have been reported.[16, 17] The subsequent transitions transform AgI from a wurtzite to a rock-salt structure, via a zinc-blende structure, to finally reach a tetragonal structure in which atoms are in octahedral coordination. In the case of CuI, several phase transitions have been found in the same pressure range.[18, 19] The structural sequence goes from the zinc-blende structure to rhombohedral, tetragonal, and cubic rock-salt phases. A tetragonal post-rock-salt structure has been reported, atoms being in a tetrahedral coordination. However, the information of HP structures provided by neutron and x-ray diffraction (XRD) experiments and theoretical calculations is contradictory.[20] Surprisingly, to

date, AuI has never been studied at HP. The scarce information on AuI concerns both high pressure and ambient conditions. This is due to the challenges to overcome the tendency of gold (Au) not to form stable bonds with any atomic element in crystalline solids. Computationally, density-functional theory (DFT) cannot explain the low-symmetry crystal structure of AuI. The calculations predict zinc-blend or rock-salt structures[21] (like those found in AgI and CuI respectively) instead of the polymeric crystal structure of AuI obtained experimentally.[22]

In order to improve the knowledge on the HP structural behavior of aurophilic metal iodides, we have studied AuI up to 13.5 GPa with synchrotron-based powder XRD. Our results reveal the shortest Au-Au aurophilic distance, 2.789 Å, reported so far in inorganic solids, at a pressure of 9.2 GPa. Moreover, we have found that in contrast with AgI and CuI counterparts only one phase transition occurs in AuI up to 10.7 GPa. We have also discovered evidence of the occurrence of a pressure-induced amorphization (PIA) beyond 10.7 GPa. We have found that the phase transition is of first-order character and involves the transformation of AuI from a polymeric layered structure into a regular three dimensional crystal structure with Au clusters. The compressibility of both structures has been determined. Details of the experiments will be given in the next section and the results will be presented and discussed in the section 'Results and discussion' of the paper.

2. EXPERIMENTAL DETAILS

For the experiments we used 99.9% purity AuI powder from Sigma-Aldrich and packed under argon. This powder contains impurities of metallic gold that give a yellow coloration. HP experiments were carried out using a membrane diamond-anvil cell (DAC) with diamond culets of 500 μm and an Inconel gasket pre-indented to 40 μm. In order to reduce the exposure to moisture and light as well as to avoid chemical reactions, AuI was loaded directly from the packing bottle

to the DAC and no pressure medium was used in the experiments. This might induce non-hydrostatic conditions, however, due to the small bulk modulus of AuI (we determined it to be 18.1(8) GPa (LP phase) and 31.8(1.5) GPa (HP phase) as we will explain latter), deviatoric stresses can be neglected in the pressure range covered by our experiments ($P \leq 13.5$ GPa).[23, 24] In order to determine pressure, we used the diffraction peaks of gold impurities as pressure standard.[25] HP angle-dispersive powder XRD measurements were carried out at room temperature at the Materials Science and Powder Diffraction beamline of ALBA Synchrotron.[26] We used a monochromatic x-ray beam ($\lambda = 0.4642$ Å) focused down to a 20 μm × 20 μm and a Rayonix CCD detector. The sample-to-detector distance (210 mm) and the beam center position were calibrated using the FIT2D software[27] with the LaB_6 diffraction pattern measured under the same conditions as the sample. During acquisition, the DAC was rocked by ±3° in order to obtain a uniform intensity distribution in the diffraction images collected at the detector. These images were integrated using DIOPTAS software[28] in order to analyze them using PowderCell[29] and FullProf[30].

3. RESULTS AND DISCUSSION

Fig. 1 shows the XRD pattern measured at ambient pressure in the DAC together with the Rietveld refinement. This structural refinement confirms the tetragonal crystal structure (space group $P4_2/ncm$) reported by Jagodzinski[22] as can be seen in the figure by the quality of the Rietveld fit and the small residuals. This structure has four formula units per unit cell ($Z = 4$). All the peaks in the XRD pattern can be assigned either to this structure or to Au. The ambient conditions unit-cell parameters determined from our experiment are $a = 4.355(3)$ Å and $c = 13.709(9)$ Å. The goodness-of-fit factors of the refinement are $R_P = 2.19$ %, $R_{WP} = 2.83$ %, and $\chi^2 = 1.16$. Regarding atomic positions in the LP phase of AuI, Au atoms are at the high-symmetry Wyckoff position 4*d* (0, 0,

0) and the iodine (I) atoms are at the position 4*e* (0.25, 0.25, 0.15302(9)), being the z coordinate of I, the only free positional parameter, which was determined from the refinement.

The crystal structure of the LP tetragonal polymorph of AuI (Fig. 2a) basically consists of -I-Au-I-Au-I- polymeric zigzag chains, which form layers oriented perpendicular to the c-axis. The Au and I atoms are bonded by means of covalent bonds. The infinite zigzag chains in the solid (Fig. 2b) are linked via Au···Au aurophilic interactions along the Au plane (a-b plane) analogous to an fcc close-packing array. Notice that within each layer there is an inversion center between parallel chains and that in neighboring layers the chains run in two perpendicular directions (Fig. 2c). The layers are held together along the c-axis by van der Waals forces amongst I atoms. At ambient pressure, the shortest interatomic distances are those of intralayer Au-I bonds shown in Fig. 2a, which is 2.602 Å, and the Au-I-Au angle in the zigzag chains is 72.42°. Within each layer, the Au atoms form an fcc-like square two-dimensional (2D) network (Fig. 2c) in which the Au-Au distance is equal to $a/\sqrt{2}$ = 3.076 Å, which is a typical distance of aurophilic bonds at ambient conditions.[6, 7] We can compare this distance with those of other aurophilic structures, e. g. in gold chloride AuCl[31], 3.22 Å, and in organometallic solids like the [1,4-C_6H_4{PPh_2(AuCl)}$_2$], 3.6686(5) Å, and in $AuEt_2DTC \cdot xCH_2Cl_2$, 2.78 Å.[11, 12] The Au-Au distance in AuI is significantly shorter than in these reported above. On the one hand, I atoms in each layer form simple square 2D networks at each side of the Au network in which the distance between I atoms is equal to the unit-cell parameter *a*; i.e. 4.355(3) Å. On the other hand, I atoms from subsequent layers are arranged in such a way that they make a regular square pyramid, where one I atom at one layer (the vertex of the pyramid) is separated from the other four I atoms in the neighboring layer (the base of the pyramid) by 4.069(3) Å (Fig. 2a). The structure of AuI can be explained by considering the metallic fcc-structure of Au in which the I has been incorporated.

Fig. 3 shows XRD patterns obtained under compression up to 4.9 GPa. As pressure increases, the typical shift of peaks towards higher angles due to the reduction of unit-cell parameters is observed. It is interesting that the (102) peak shifts faster than the (002) and (004) peaks, thus indicating that the compression of the crystal is anisotropic. Indeed, the (102) peak gradually approaches the (004) peak as can be seen in the figure. At 1.5 GPa, a few new peaks can be detected. They are identified with asterisks in the figure. As pressure increases, the new peaks become more intense. These peaks are the evidence of the onset of a structural phase transition. From 1.5 to 3.3 GPa, the LP phase and the new HP phase coexist. At 3.8 and 4.9 GPa, the XRD patterns have been indexed only with the novel HP phase; therefore, the phase transition to the HP phase is already completed at 3.8 GPa.

The pressure evolution of distances of the LP and HP phase is represented in Fig. 4. Such distances were calculated through the atomic positions obtained by Rietveld refinement, being the z coordinate of I atoms, the only atomic coordinate in the fitting. At 3.3 GPa, the highest pressure where the LP phase is still detected, the Au-I distance has been reduced from the ambient pressure value of, 2.602 Å, to 2.499 Å (Fig. 4b). On the other hand, the intralayer and interlayer I-I distances have been compressed from 4.350 and 4.069 Å to 4.076 and 3.874 Å, respectively (Fig. 4c). Interestingly, at 3.3 GPa, the Au-Au distance is 2.882 Å (Fig. 4a); i.e. the same interatomic distance as in the fcc structure of gold at ambient pressure, the tetragonal phase of AuI retains the square lattice of fcc-Au, but with expanded Au-Au distances due to the incorporation of I atoms in the structure of Au metal. Recently, a close-packing array of Sn atoms, like those present in pure fcc-Sn, has been found in $CaCl_2$-type SnO_2. This supports the argument that the cation array is the major factor governing structure formation and evolution under pressure.[32] These examples cannot be a mere coincidence and seem to provide support to the "anions in metallic matrices" model.[33]

From the XRD patterns collected at 3.8 and 4.9 GPa we have determined a tentative crystal structure for the HP phase of AuI. Fig. 1 shows the pattern measured at 4.9 GPa and the results of a Rietveld refinement. In order to find a candidate for the crystal structure of the HP phase, first, we have indexed the XRD pattern using DICVOL[34] and assigned the low-angle region of the pattern, where there is no overlap of the AuI peaks, with those of Au.[35] We have obtained the highest figure of merit for a monoclinic unit cell (space group *P*2/*m*) with a = 11.159(9) Å, b = 13.208(9) Å, c = 4.229(3) Å, β = 95.67(5)°. The unit-cell volume indicates that the crystal structure has Z = 12 and it contains 6 I atoms and 3 Au atoms in non-equivalent positions labelled I1, I2, I3, I4, I5, I6, Au1, Au2, and Au3, respectively. Subsequently, by applying the Le Bail method,[36] we confirmed that quite a good fit is obtained when using the above described monoclinic unit-cell. Then, the crystal structure was estimated by direct methods using the integrated intensities.[37] Afterwards, the XRD pattern was quantitatively analyzed using the Rietveld refinement method.[38] After background subtraction, the overall scale-factor, unit-cell, and line-shape parameters were refined. Then, the atomic positions were subsequently determined. In order to reduce the number of free parameters used in the refinement, the occupancy (SOF) and overall atomic displacement factors (B) were constrained to SOF = 1 and B = 0.5 Å^2.[39, 40] The small residuals of Rietveld refinement reveal that the profile fitting quality is good. The refined structural parameters are given in Table 1. The parameters describing the goodness of fit in the Rietveld refinement are R_P = 3.01 %, R_{WP} = 3.76 %, and χ^2 = 2.22. Therefore, we consider that we have found a plausible crystal structure for the HP phase, taking into account the quality of XRD patterns of the HP phase, which were spotty in spite of the 6º rocking used in the experiments. Regrettably, a better crystallinity of the sample could not be achieved by warming the sample because it would likely decompose as happen with other gold halide compounds. Moreover, unfortunately, this structure cannot be

confirmed by density-functional calculations for the moment because they do not reproduce properly the structure of any gold compound due to the relativistic nature of the Au atoms and its tendency of forming Au-Au bonds through aurophilic interactions (interactions between its filled 5d orbitals). We would like to mention here that from the relative intensity of gold peaks, we discard the partial decomposition of AuI after the phase transition since we did not notice any increase of the contribution of metallic phase of Au detected initially in the starting sample. The crystal structure of the proposed HP phase is schematically represented in Fig. 5.

There, it can be seen that the phase transition involves changes in the pattern of chemical bonds, being therefore a reconstructive (first-order) transformation.[41] The first-order nature of the transition is consistent with the fact that there is a sudden volume collapse associated with it. From our experiments, we determined the volume per-formula-unit of the LP phase to be 73.9(2) Å at 3.3 GPa and that of the HP phase to be 70.1(2) Å at 3.8 GPa. Therefore, the relative collapse of the volume ($\Delta V/V$) is around 5 %. By comparing Fig. 2a with Fig. 5, it can be clearly seen the transformation is from the crystal structure from a 2D polymeric crystal to a conventional 3D crystal.

In the HP structure there is a mirror plane at $y = 0.5$ which contains I atoms. There is a second mirror plane at $x = 0.5$. There are also several "empty" cavities; like the hexagonal cavities that can be seen in Fig. 5. The structure can be seen as a host-guest structure,[42] comprising a host framework of I atoms and an Au cluster guest, forming Au1··Au2··Au3··Au1··Au2 chains. In such a structure, Au1 atoms are fourfold coordinated with two Au atoms and two I atoms, Au2 atoms are threefold coordinated with two Au atoms and Au3 atoms are fivefold coordinated by two Au atoms and three I atoms (Fig. 5).

The pressure evolution of the distances in the HP phase can be seen in Fig. 4. They have been calculated by using the lattice parameters at each pressure obtained by LeBail fitting and fixing the atomic positions obtained through a Rietveld refinement at 4.9 GPa. This procedure has been carried out in this way due to difficulty of fit all the 9 non-equivalent atomic positions the HP phase. At 4.9 GPa, the Au-Au distances are 2.845 Å for the Au1-Au2 bonds, 2.959 Å for Au1-Au3 bonds and 3.051 Å for Au2-Au3 bonds. The average Au-I distances is 2.732 Å. Some Au-I distances are slightly larger in the HP phase (Fig. 4b). Contrastingly, the smallest Au-Au distances are shorter than these in the LP phase and they are comparable to the Au-Au distances, 2.9 Å, in the metallic Au phase. The aurophilic bonds shorten by 0.29 Å, from 3.076 at 0 GPa to the shortest Au-Au distance (Au1-Au2) of 2.789 Å at 9.2 GPa (Fig. 4a). To the best of our knowledge, this is the shortest pressure-induced Au-Au aurophilic distance in a 3D fully inorganic structure and the largest pressure-induced contraction in the length of an aurophilic interaction within just 9.2 GPa. Damian Paliwoda *et al*. reported the pressure-induced shortening of aurophilic contacts, from 2.78 Å to 2.72 Å, in the organometallic gold(I) diethyldithiocarbamate polymer (organometallic solid) between 0 and 1 GPa and Alice E. O'Connor *et al*. published the largest pressure-induced contraction in the length of an aurophilic interaction, 0.613 Å, obtained from 0 to 10.6 GPa in another organometallic compound, [1,4-C_6H_4{$PPh_2(AuCl)$}$_2$].[11, 12]

Fig. 4c shows that the I-I distances in the HP phase vary from 2.244 to 2.984 Å. The most of these distances are similar to those of the HP phase of solid iodine.[43] However for the case of AuI they occur at 4.9 GPa instead of the 12 GPa required in pure iodine. Therefore, the new high-pressure phase of AuI is dominated by Au-I and I-I covalent bonds and Au-Au aurophilic bonds. It is noticeable that such a phenomenon has never been seen before in any of the polymorphs of AgI and CuI.[14-19]

The present discovery of a transition in AuI from a polymeric 2D solid to a covalent 3D crystal delineates a picture for the HP behavior of aurophilic compounds, which could have significant consequences on their investigation. The formation of I-I bonds could probably have consequences in the electronic band structure of AuI. Indeed, a color change is observed in AuI (from yellow to dark gray) at the phase transition, which is consistent with a substantial reduction of the electronic band gap.[44, 45] Notice that the same phenomenon has been observed in layered materials when pressure induces a transition from a 2D to a 3D structure.[46, 47] This phenomenon can be ascribed to the formation of resonant bonding of halogen atoms due to increase of coordination.[48]

Upon further compression, we found the HP phase to remain stable up to 10.7 GPa. In Fig. 6, we show XRD patterns measured from 4.9 to 13.5 GPa. There, it can be seen that the most relevant change from 4.9 to 10.7 GPa is the gradual shift of Bragg reflections towards higher angles due to the decrease of the d-spacing as consequence of the compression of the unit-cell. In addition, there is a merging of the two most intense peaks (located near $2\theta = 9°$), which is caused by the decrease of the β angle, a fact that we will comment on later. At 9.9 and 10.7 GPa a broadening of the peaks is observed probably due to non-hydrostatic effects (remember that no pressure medium is used). However, the XRD patterns can be satisfactorily explained with the proposed HP phase. Beyond 10.7 GPa we observed the XRD peaks further broaden and the intensities of them diminish, many of them disappearing.

Such a phenomenon is enhanced with pressure. It is accompanied by an increase in the background in the 9-13° region. Indeed, at 13.5 GPa, the XRD pattern basically consists of only the two Au peaks and two additional broad bands located near 9-10°. Interestingly, this process is irreversible and resembles a PIA.[49, 50] The broad bands in the XRD patter correspond to distances of 2.75 and 3.00 Å. They can be associated with interatomic distances in the disordered phase. The causes of

disordering can be mechanical or vibrational instabilities (from the material itself or caused by the non-hydrostaticity) or even the presence of large kinetic barriers blocking the transition to a second crystalline HP phase.[51, 52] From our experiments we have obtained the pressure dependence of the unit-cell parameters of the two polymorphs of AuI (Fig. 7).

For the case of the LP phase, results are provided up to 3.3 GPa, while for the HP phase they have been obtained from 3.8 to 10.7 GPa. In the LP phase, the pressure dependence for both unit-cell parameters is nearly linear, but the compressibility is anisotropic, the c-axis being the less compressible. The axial compressibilities at ambient pressure in the different crystallographic directions, $k_x = (-1)/x \ \partial x/\partial P$, yield k_a = 1.98 10^{-2} GPa^{-1} and k_c = 9.76 10^{-3} GPa^{-1}. Since $k_a \cong 2\ k_c$, the tetragonal AuI is more compressible along the layers than in the direction perpendicular to the layers. This behavior is expected since the contribution of the Au-I covalent bond is stronger along the c-axis than in the a-b plane. From the axial compressibilities, the bulk modulus (B_0) can be determined as $B_0 = 1/(2\ k_a + k_c\ )$ being its value 20 GPa.

In contrast with the behavior found for the LP phase, in the HP monoclinic phase the compressibility is similar along the three crystallographic directions. Moreover, they are of the same order than k_c in the LP phase. The relative changes with pressure of a, b, and c in the HP phase are basically the same as in c for the LP phase (Fig. 7). This is due to the fact that in the HP phase, the contribution of Au-I covalent bonds is similar in all directions of the unit cell and the I-I covalent bonds contribute in the a-c plane. On the other hand, the monoclinic β angle is drastically reduced by pressure following a quadratic pressure dependence (Fig. 7).

In Fig. 7, we also represent the pressure dependence of the unit-cell volume. In the figure it can be seen that the HP polymorph is less compressible than the LP one, as expected. It can also be

observed the volume collapse that occurs at the phase transition. From these results we have determined room-temperature P-V equations of state (EOS) for the two phases. We have found that the pressure dependence of the unit-cell volume can be properly reproduced by a third-order Birch-Murnaghan EOS.[53, 54] For the LP phase, we have determined the unit-cell volume at ambient pressure (V_0), bulk modulus (B_0), and its pressure derivative (B_0'). Their values are: V_0 = 259.8(5) Å^3, B_0 = 18.1(8) GPa, and B_0' = 2.0(4). The fitted EOS is shown in Fig. 7. The maximum deviation between the experimental pressure and that determined from the EOS is only 0.1 GPa, which indicates that the obtained EOS has an excellent predictive capability. Notice that the bulk modulus is similar to that determined from the linear compressibilities, indicating that most of the compression of the structure occurs along the layers. In addition, B_0 has a very small value, comparable to that of rare-gas solids[55] and molecular solids[23], and 50% smaller than the bulk modulus of the different polymorphs of AgI and CuI.[56, 57, 58] On the other hand, this B_0 is of the same order as that of the aurophilic organometallic solid [1,4-C_6H_4{PPh_2(AuCl)}$_2$], which is 8(13) GPa.[11] Moreover, the pressure derivative of the bulk modulus is much smaller than the typical value for this parameter, which is expected to be near 4 in ionic-covalent solids.[59] Curiously, the pressure derivative in many highly compressible molecular solids and open framework structures based on van der Waals interatomic bonds is usually much higher than 4,[23, 48, 60] thus reflecting a strong increase of the strength of van der Waals interactions with increasing pressure. Therefore, the small value of the pressure derivative of AuI could be ascribed to the soft nature of intralayer Au-Au bonds. In summary, both the van der Waals interactions and Au-Au interactions make the 2D polymeric polymorph of AuI an unusually highly compressible solid.

Regarding the HP phase of AuI, we have determined the following EOS parameters: V_0 = 700.4(9) Å^3, B_0 = 31.8(15) GPa, B_0' = 3.9(1.1). The fitted EOS is shown in Fig. 7. In this case, the maximum

deviation between the measured and calculated pressure from the EOS is 0.25 GPa, which shows that the obtained EOS properly represents the pressure dependence of volume. It can be seen that in the HP phase there is a large increase in both B_0 and B_0' as compared with the LP phase. In fact, B_0' becomes similar to 4 as usual in crystalline ionic-covalent solids[48] and B_0 becomes comparable to the bulk modulus of AgI and CuI.[23-33] The substantial decrease of the compressibility of AuI in the HP phase is consistent with the volume collapse associated with the phase transition, the reduction of interatomic distances and the formation of additional chemical bonds of ionic-covalent character.

4. CONCLUSIONS

We have performed a high-pressure study of the structural properties of AuI up to 13.5 GPa. The crystal structures at different pressures have been determined using a diamond-anvil cell and synchrotron powder x-ray diffraction. We have rigorously studied the effects of compression in the crystal structure finding the existence of a first-order phase transition at 3.8 GPa (the onset being at 1.5 GPa) followed by a disordering at 11.5 GPa. The crystal structure of the new polymorph has been determined and tentatively assigned to a monoclinic space group ($P2/m$). In addition, we have obtained information on the axial and bulk compressibility of the LP and HP phases of AuI. From these results, the room-temperature EOS has been obtained for both phases. The LP phase is extremely compressible, being as soft as a rare-gas or a molecular solid. The compressibility is reduced in the HP phase, becoming similar to that of other noble metal iodides. Moreover, we report the shortest Au-Au aurophilic distance, 2.789 Å at 9.2 GPa, and the largest pressure-induced contraction in the length of an aurophilic interaction, 0.29 Å, in the pressure

range, from 0 to 9.2 GPa, in a 3D fully inorganic Au^{+} complex. The obtained information of the high-pressure behaviour of the crystal structure is useful to get valuable microscopic insights into the superionic features of noble-metal iodides, required to improve the knowledge on the barocaloric properties of these compounds, which are governed by pressure-driven structural phase transitions involving large entropy changes related to the displacement of iodine ions. [61, 62]

ACKNOWLEDGEMENTS

The authors thank the financial support of the Spanish Ministerio de Ciencia, Innovación y Universidades, the Spanish Research Agency (AEI), and the European Fund for Regional Development (FEDER) under Grant No. MAT2016-75586-C4-1/2-P and by Generalitat Valenciana under Grant Prometeo/2018/123 (EFIMAT). J.A.S. acknowledges the "Ramón y Cajal" fellowship program (RYC-2015-17482) and Spanish Mineco Project FIS2017-83295-P. V. M. acknowledges the "Juan de la Cierva" program (FJCI-2016-27921) for financial support. Experiments were performed at the Materials Science and Powder Diffraction beamline of ALBA Synchrotron. The authors thank the collaboration of ALBA staff. We also thank D. Santamaría-Pérez for fruitful discussions.

REFERENCES

[1] H.-K. Mao, X.-Y Chen, Y. Ding, B. Li and L. Wang. Solids, liquids, and gases under high pressure. Rev. Mod. Phys., 2018, 90, 015007.

[2] A. Benmakhlouf, D. Errandonea, M. Bouchenafa, S. Maabed, A. Bouhemadoud and A. Bentabete. New pressure-induced polymorphic transitions of anhydrous magnesium sulfate. Dalton Trans., 2017, 46, 5058.

[3] E. Horvath-Bordon, R. Riedel, A. Zerr, P. F. McMillan, G. Auffermann, Y. Prots, W. Bronger, R. Kniep and P. Kroll. High-pressure chemistry of nitride-based materials. Chem. Soc. Rev., 2006, 35, 987.

[4] D. Errandonea and A. B. Garg. Recent progress on the characterization of the high-pressure behaviour of AVO4 orthovanadates. Progress in Materials Science, 2018, 97, 123.

[5] F. J. Manjon and D. Errandonea. Pressure-induced structural phase transitions in materials and earth sciences. Phys. Stat. Sol. B, 2009, 246, 9.

[6] Angel Vegas. Cations in Inorganic Solids. Crystallography Reviews, 2000, 7:3, 189.

[7] Hubert Schmidbaur. The aurophilicity phenomenon: A decade of experimental findings, theoretical concepts and emerging applications. Gold Bulletin, 2000, 33, 3.

[8] Robert E. Bachman, Michael S. Fioritto, Susan K. Fetics, and T. Matthew Cocker. The Structural and Functional Equivalence of Aurophilic and Hydrogen Bonding: Evidence for the First Examples of Rotator Phases Induced by Aurophilic Bonding. J. Am. Chem. Soc., 2001, 123, 5376.

[9] Pekka Pyykkö. Strong Closed-Shell Interactions in Inorganic Chemistry. Chem. Rev., 1997, 97, 597.

[10] Nino Runeberg, Martin Schütz and Hans-Joachim Werner. The aurophilic attraction as interpreted by local correlation methods. J. Chem. Phys., 1999, 110, 7210.

[11] Alice E. O'Connor, Nedaossadat Mirzadeh, Suresh K. Bhargava, Timothy L. Easun, Martin Schröder and Alexander J. Blake. Aurophilicity under pressure: a combined crystallographic and in situ spectroscopic study. Chem. Commun., 2016, 52, 6769.

[12] Damian Paliwoda, Paulina Wawrzyniak and Andrzej Katrusiak. Unwinding $Au^{+}\cdots Au^{+}$ Bonded Filaments in Ligand-Supported Gold(I) Polymer under Pressure. J. Phys. Chem. Lett., 2014, 5, 2182.

[13] C. Cazorla and D. Errandonea. Giant Mechanocaloric Effects in Fluorite-Structured Superionic Materials. Nano Lett., 2016, 16, 3124.

[14] A. Aznar, P. Lloveras, M. Romanini, M. Barrio, J. L. Tamarit, C. Cazorla, D. Errandonea, N. D. Mathur, A. Planes, X. Moya and L. Mañosa. Giant barocaloric effects over a wide temperature range in superionic conductor AgI. Nature Commun., 2017, 8, 1851.

[15] A. K. Sagotra, D. Errandonea and C. Cazorla. Mechanocaloric effects in superionic thin films from atomistic simulations. Nature Commun., 2017, 8, 963.

[16] D. A. Keen, S. Hull, W. Hayes and N. J. G Gardner. Structural Evidence for a Fast-Ion Transition in the High-Pressure Rocksalt Phase of Silver Iodide. Phys. Rev. Lett., 1996, 77, 4914.

[17] O. Ohtaka, H. Takebe, A. Yoshiasa, H. Fukuia and Y. Katayama. Phase relations of AgI under high pressure and high temperature. Solid State Commun., 2002, 123, 213.

[18] S. Hull and D. A. Keen. High-pressure polymorphism of the copper(I) halides: A neutron-diffraction study to ~10 GPa. Phys. Rev. B, 1994, 50, 5868.

[19] A. Blacha, N. E. Christensen and M. Cardona. Electronic structure of the high-pressure modifications of CuCl, CuBr, and CuI. Phys. Rev. B, 1986, 33, 2413.

[20] J. Zhu, R. Pandey and M. J. Gu. The phase transition and elastic and optical properties of polymorphs of CuI. Phys.: Condens. Matter, 2012, 24, 475503.

[21] T. Söhnel, H. Hermann and P. J. Schwerdtfeger. Solid state density functional calculations for the group 11 monohalides. Phys. Chem. B., 2005, 109, 526.

[22] H. Jagodzinski. Die Kristallstruktur des AuJ. Zeitschrift für Kristallographie, 1959, 112, 80.

[23] J. A. Sans, F. J. Manjón, C. Popescu, A. Muñoz, P. Rodríguez-Hernández, J. L. Jordá and F. J. Rey. Arsenolite: a quasi-hydrostatic solid pressure-transmitting medium. Physics: Condensed Matter, 2016, 28, 475403.

[24] D. Errandonea, A. Muñoz and J. Gonzalez-Platas. High-pressure x-ray diffraction study of YBO_3/Eu^{3+}, $GdBO_3$, and $EuBO_3$: Pressure-induced amorphization in GdBO3. J. Appl. Phys., 2014, 115, 216101.

[25] K. Hirose, N. Sata, T. Komabayashi and Y. Ohishi. Simultaneous volume measurements of Au and MgO to 140 GPa and thermal equation of state of Au based on the MgO pressure scale. Phys. Earth Planet. Inter., 2008, 167, 149.

[26] F. Fauth, I. Peral, C. Popescu and M. Knapp. The new Material Science Powder Diffraction beamline at ALBA Synchrotron. Powder Diffr., 2013, 28, S360.

[27] A. P. Hammersley, S. O. Svensson, M. Hanfland, A. N. Fitch and D. Häusermann. Two-dimensional detector software: From real detector to idealized image or two-theta scan. High Pressure Res., 1996, 14, 235.

[28] C. Prescher and V. B. Prakapenka. DIOPTAS: a program for reduction of two-dimensional X-ray diffraction data and data exploration. High Press. Res., 2015, 35, 223–230.

[29] W. Kraus and G. J. Nolze. POWDER CELL - a program for the representation and manipulation of crystal structures and calculation of the resulting X-ray powder patterns. J. Appl. Crystal., 1996, 29, 301.

[30] J. Rodrıguez-Carvajal. Recent advances in magnetic structure determination by neutron powder diffraction. Phys. B, 1993, 192, 55.

[31] Klaus Doll, Pekka Pyykkö, and Hermann Stoll Closed-shell interaction in silver and gold chlorides. J. Chem. Phys., 1998, 109, 6.

[32] H. T. Girao, P. Hermet, B. Masenelli, J. Haines, P. Mélinon and D. Machon. Pressure-Induced Sublattice Disordering in SnO_2: Invasive Selective Percolation. Phys. Rev. Lett., 2018, 120, 265702.

[33] A. Vegas, D. Santamaría-Pérez, M. Marqués, M. Florez, V. García Baonza and J. M. Recio. Anions in metallic matrices model: application to the aluminium crystal chemistry. Acta Crystallogr. Sect. B, 2006, 62, 220.

[34] A. Boultif and D. J. Louër. Powder pattern indexing with the dichotomy method. J. Appl. Crystal., 1991, 24, 987.

[35] D. Errandonea. Exploring the properties of MTO_4 compounds using high-pressure powder x-ray diffraction. Cryst. Res. Tech., 2015, 50, 729.

[36] A. Le Bail, H. Duroy and J. L. Fourquet. Ab-initio structure determination of LiSbWO6 by X-ray powder diffraction. Mater. Res. Bull., 1988, 23, 447.

[37] A. Altomare, C. Giacovazzo, A. G. G. Moliterni and R. Rizz. Direct Methods Optimised for Solving Crystal Structure by Powder Diffraction Data: Limits, Strategies, and Prospects. J. Res. Natl. Inst. Stand. Technol., 2004, 109, 125.

[38] H. M. Rietveld. A profile refinement method for nuclear and magnetic structures. J. Appl. Cryst., 1969, 2, 65.

[39] D. Errandonea, O. Gomis, B. García-Domene, J. Pellicer-Porres, V. Katari, S. N. Achary, A. K. Tyagim and C. Popescu. New Polymorph of $InVO_4$: A High-Pressure Structure with Six-Coordinated Vanadium. Inorg. Chem., 2013, 52, 12790.

[40] D. Errandonea, R. S. Kumar, O. Gomis, F. J. Manjón, V. V. Ursaki and I. M. Tiginyanu. X-ray diffraction study on pressure-induced phase transformations and the equation of state of $ZnGa_2Te_4$. J. Applied Phys., 2013, 114, 233507.

[41] P. Tolédano and V. Dmitriev, Reconstructive Phase Transitions in Crystals and Quasicrystals, World Scientific, London, 1996.

[42] M. I. McMahon, S. Rekhi and R. J. Nelmes. Pressure Dependent Incommensuration in Rb-IV. Phys. Rev. Lett., 2001, 87, 055501.

[43] Q. Zeng, Z. He, X. San, Y. Ma, F. Tian, T. Cui, B. Liu, G. Zou and H.-K. Mao. A new phase of solid iodine with different molecular covalent bonds. PNAS, 2008, 105, 4999.

[44] D. Errandonea, E. Bandiello, A. Segura, J. J. Hamlin, M. B. Maple, P. Rodriguez-Hernandez and A. Muñoz. Tuning the band gap of PbCrO4 through high-pressure: Evidence of wide-to-narrow semiconductor transitions. J. Alloys Compd., 2014, 587, 14.

[45] D. Errandonea and J. Ruiz-Fuertes. A Brief Review of the Effects of Pressure on Wolframite-Type Oxides. Crystals, 2018, 8, 71.

[46] F. J. Manjón, D. Errandonea, A. Segura, J. C. Chervin and V. Muñoz. Precursor effects of the Rhombohedral-to-Cubic Phase Transition in Indium Selenide. High Pressure Research, 2002, 22, 261.

[47] V. P. Cuenca-Gotor, J. A. Sans, J. Ibáñez, C. Popescu, O. Gomis, R. Vilaplana, F. J. Manjón, A. Leonardo, E. Sagasta, A. Suárez-Alcubilla, I. G. Gurtubay, M. Mollar and A. Bergara. Structural, Vibrational, and Electronic Study of α-As_2Te_3 under Compression. J. Phys. Chem. C, 2016, 120, 19340.

[48] M. Xu, S. Jakobs, R. Mazzarello, J.-Y. Cho, Z. Yang, H. Hollermann, D. Shang, X. S. Miao, Z. H. Yu, L. Wang and M. Wuttig. Impact of Pressure on the Resonant Bonding in Chalcogenides. J. Phys. Chem. C, 2017, 121, 25447.

[49] A. L. J. Pereira, D. Errandonea, A. Beltran, L. Gracia, O. Gomis, J. A. Sans, B. Garcıa-Domene, A. Miquel-Veyrat, F. J. Manjon, A. Muñoz and C. Popescu. Structural study of α-Bi2O3 under pressure. J. Phys.: Condens. Matter, 2013, 25, 475402.

[50] A. K. Arora, T. Sato, T. Okada and T. Yagi. High-pressure amorphous phase of vanadium pentaoxide. Phys. Rev. B, 2012, 85, 094113.

[51] D. Errandonea, M. Somayazulu, and D. Häusermann. Phase transitions and amorphization of $CaWO_4$ at high pressure. Phys. Stat. Sol. B, 2003, 235, 162.

[52] H.-K. Mao, B. Chen, J. Chen, K. Li, J.-F Lin, W. Yang and H. Zheng. Recent advances in high-pressure science and technology. Matter and Radiation at Extremes, 2016, 1, 59.

[53] F. Birch. Finite strain isotherm and velocities for single-crystal and polycrystalline NaCl at high pressures and 300K. J. Geophys. Res., 1978, 83, 1257.

[54] R. J Angel. Equations of State. Rev. Mineral. Geochem., 2000, 41, 35.

[55] D. Errandonea, R. Boehler, S. Japel, M. Mezouar and L. R. Benedetti. Structural transformation of compressed solid Ar: An x-ray diffraction study to 114 GPa. Phys. Rev. B, 2006, 73, 092106.

[56] S. Hull and D. A. Keen. Pressure-induced phase transitions in AgCl, AgBr, and AgI. Phys. Rev. B, 1999, 59, 750.

[57] R. K. Singh and D. C. Gupta. Phase transition and high-pressure elastic behavior of copper halides. Phys. Rev. B, 1989, 40, 11278.

[58] D. C. Gupta and R. K. Singh. Pressure-induced phase transitions in silver halides. Phys. Rev. B, 1991, 43, 11185.

[59] A. M. Hofmeister. Pressure derivatives of the bulk modulus. J. Geophys. Res., 1991, 96, 21893.

[60] A. L. J. Pereira, J. A. Sans, R. Vilaplana, O. Gomis, F. J. Manjón, P. Rodríguez-Hernández, A. Muñoz, C. Popescu and A. Beltrán. Isostructural Second-Order Phase Transition of β-Bi_2O_3 at High Pressures: An Experimental and Theoretical Study. J. Phys. Chem. C, 2014, 118, 23189.

[61] Juan M. Bermúdez-García, Manuel Sánchez-Andújar and María A. Señarís-Rodríguez. A New Playground for Organic–Inorganic Hybrids: Barocaloric Materials for Pressure-Induced Solid-State Cooling. J. Phys. Chem. Lett., 2017, 8, 4419.

[62] Claudio Cazorla, Arun K. Sagotra, Meredith King. High-Pressure Phase Diagram and Superionicity of Alkaline Earth Metal Difluorides. J. Phys. Chem. C, 2018, 122, 1267.

Corresponding Author

*Email: virginia.monteseguro@uv.es

Author Contributions

The manuscript was written through contributions of all authors. All authors have given approval to the final version of the manuscript.

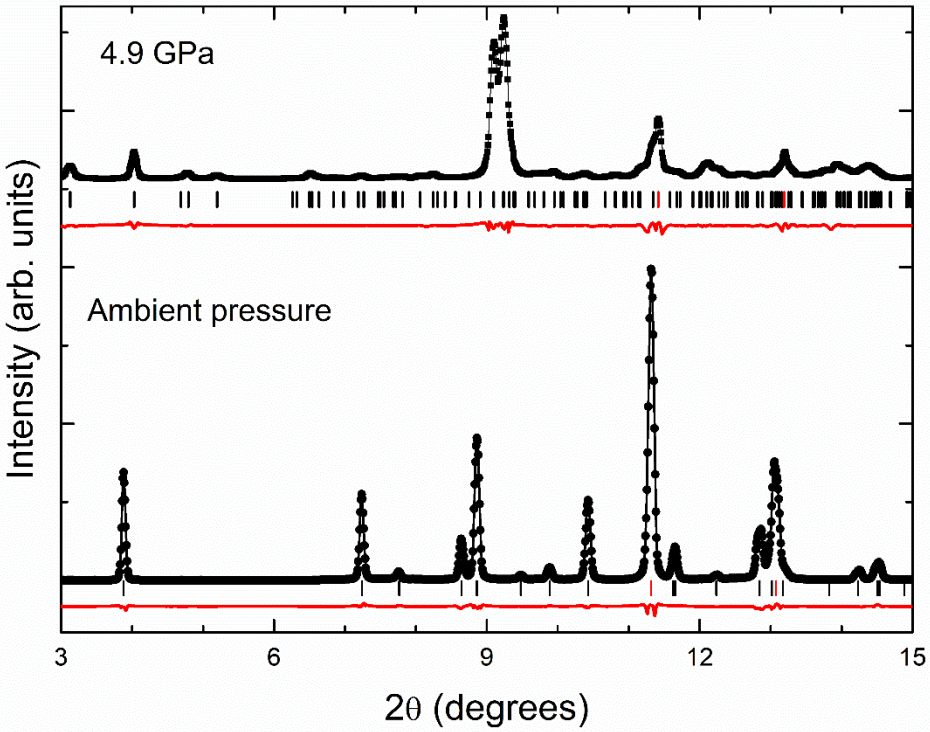

Figure 1. Background subtracted powder XRD pattern of tetragonal AuI at ambient conditions and at 4.9 GPa. The experiments are represented with dots. The black (red) solid line shows the refinement (residual). The black (red) ticks are positions of Bragg peaks of AuI (Au).

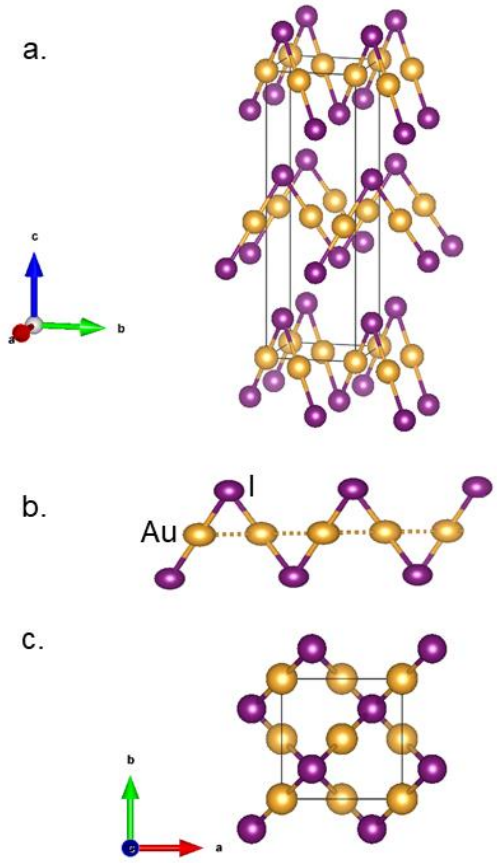

Figure 2. (a and c) Schematic views from different perspectives of the crystal structure of LP phase of AuI. (b) Infinite chain linked via Au···Au interaction. I atoms are represented as violet balls and the Au atoms as yellow balls.

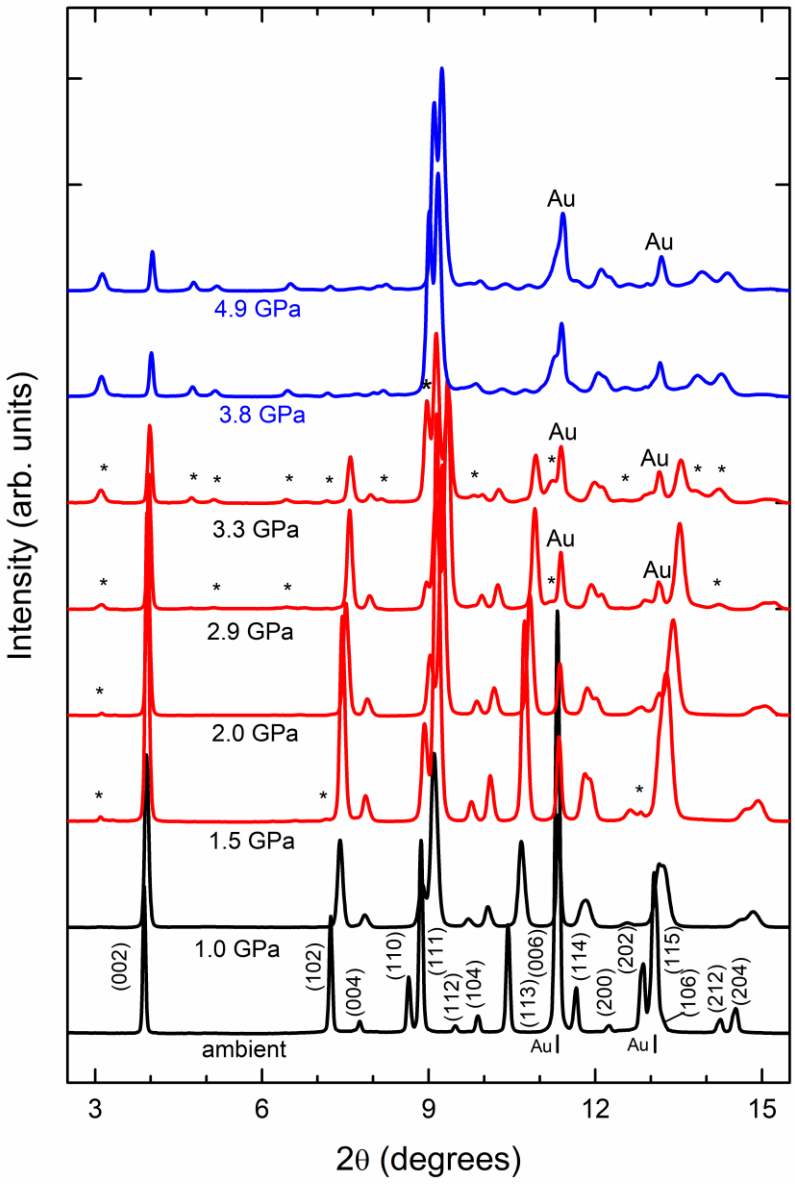

Figure 3. Selected XRD patterns of AuI measured from ambient pressure up to 4.9 GPa. The patterns at the two lowest pressures (black lines) can be assigned to the LP phase. From 1.5 to 3.3 GPa (red lines) new peaks appear, which are denoted by asterisks. Patterns at 3.8 and 4.9 GPa (blue lines) belongs to the novel HP phase. The peaks from Au are labelled. In the ambient-pressure pattern (lowest trace) the peaks of tetragonal AuI are indexed.

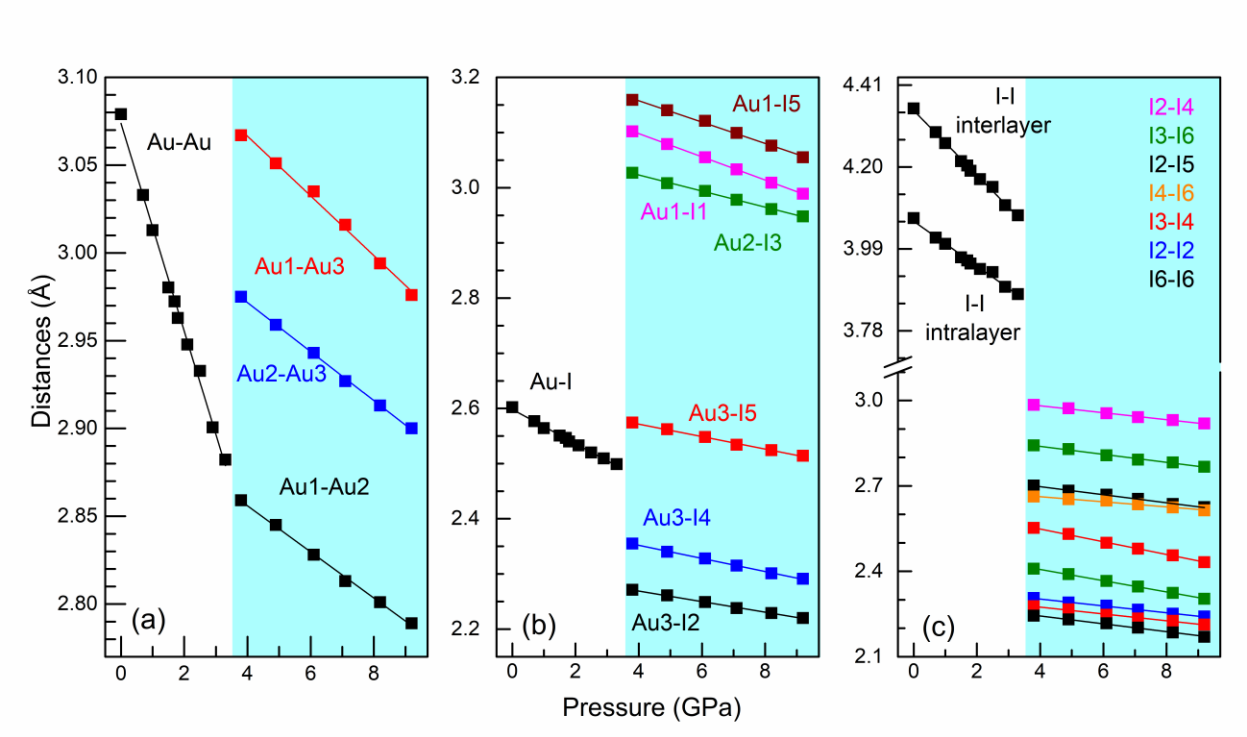

Figure 4. Pressure evolution of distances of the LP and HP phase of AuI from 0 to 9.2 GPa. (a) Au-Au distances, (b) Au-I distances and (c) I-I distances.

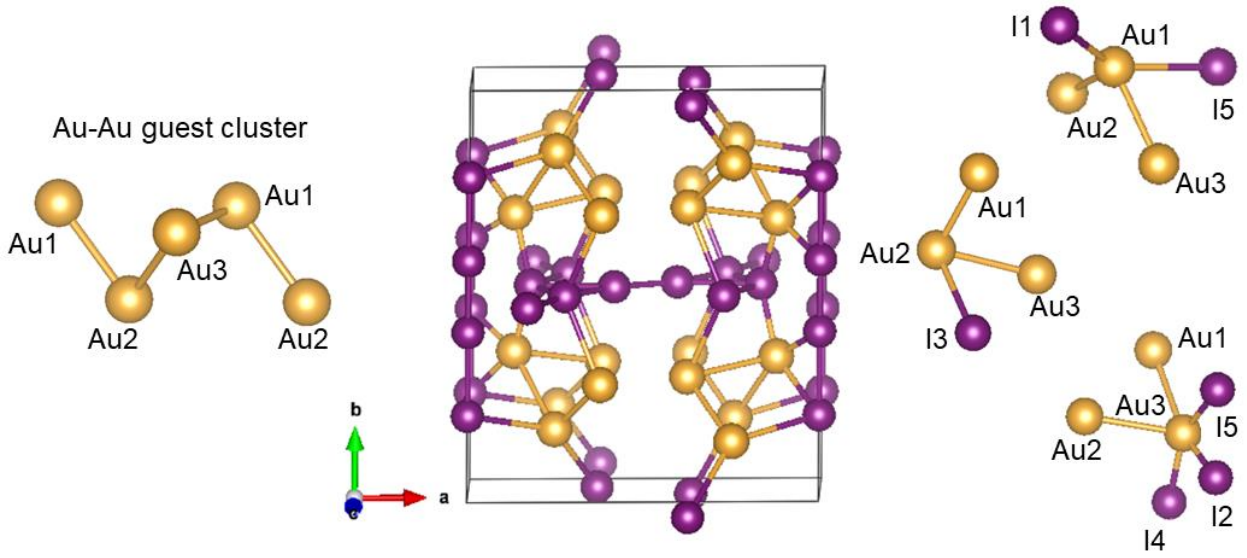

Figure 5. High-pressure phase of AuI at 4.9 GPa. It is formed by a framework of I atoms (violet) and guest clusters of Au atoms (yellow). These clusters consist of Au1··Au2··Au3··Au1··Au2 chains. The molecular units due to Au-I covalent bonds that constitute the structure are also shown.

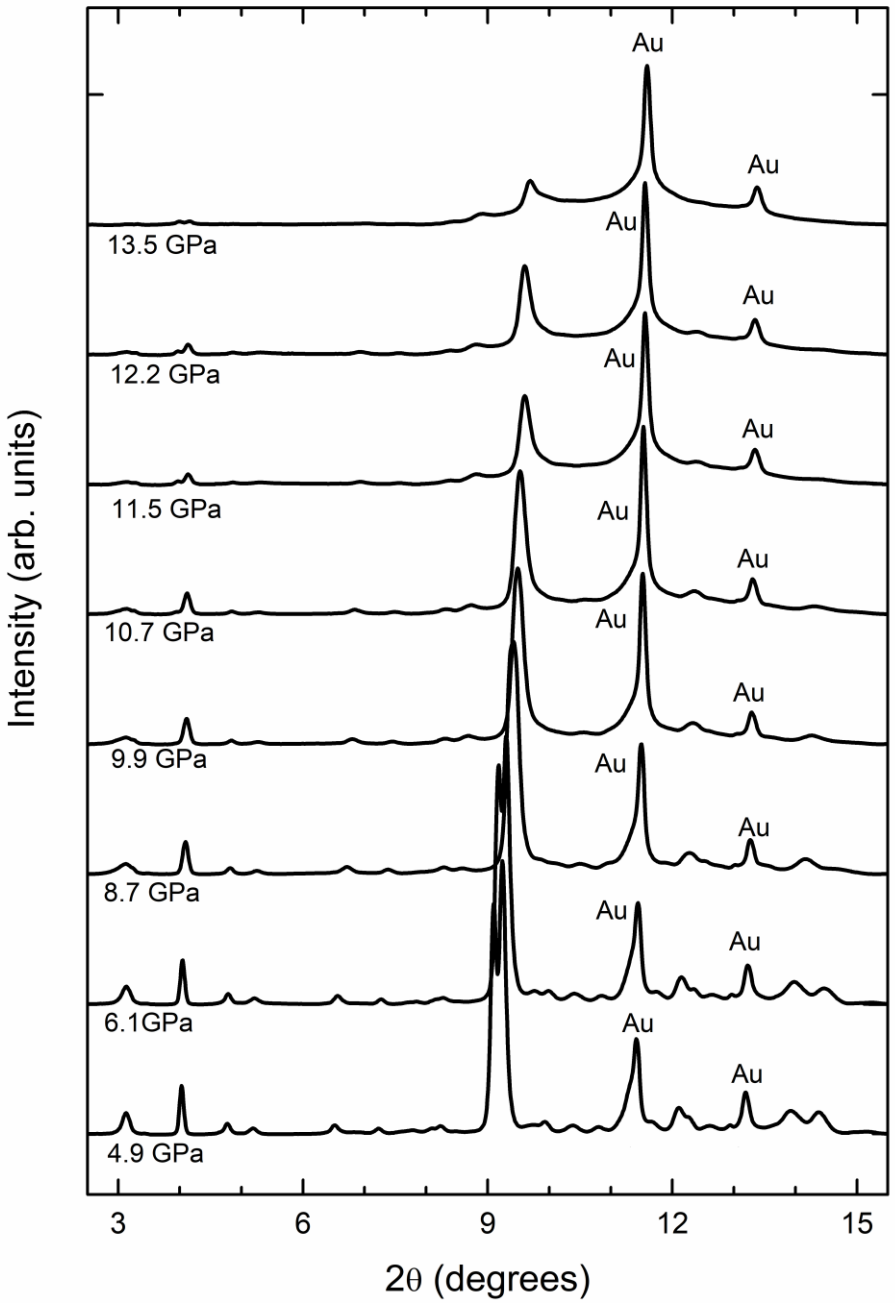

Figure 6. Selected XRD patterns of AuI measured from 4.9 to 13.5 GPa. All patterns can be assigned to the HP phase. Pressures are indicated in the figure and the peaks from Au are labelled.

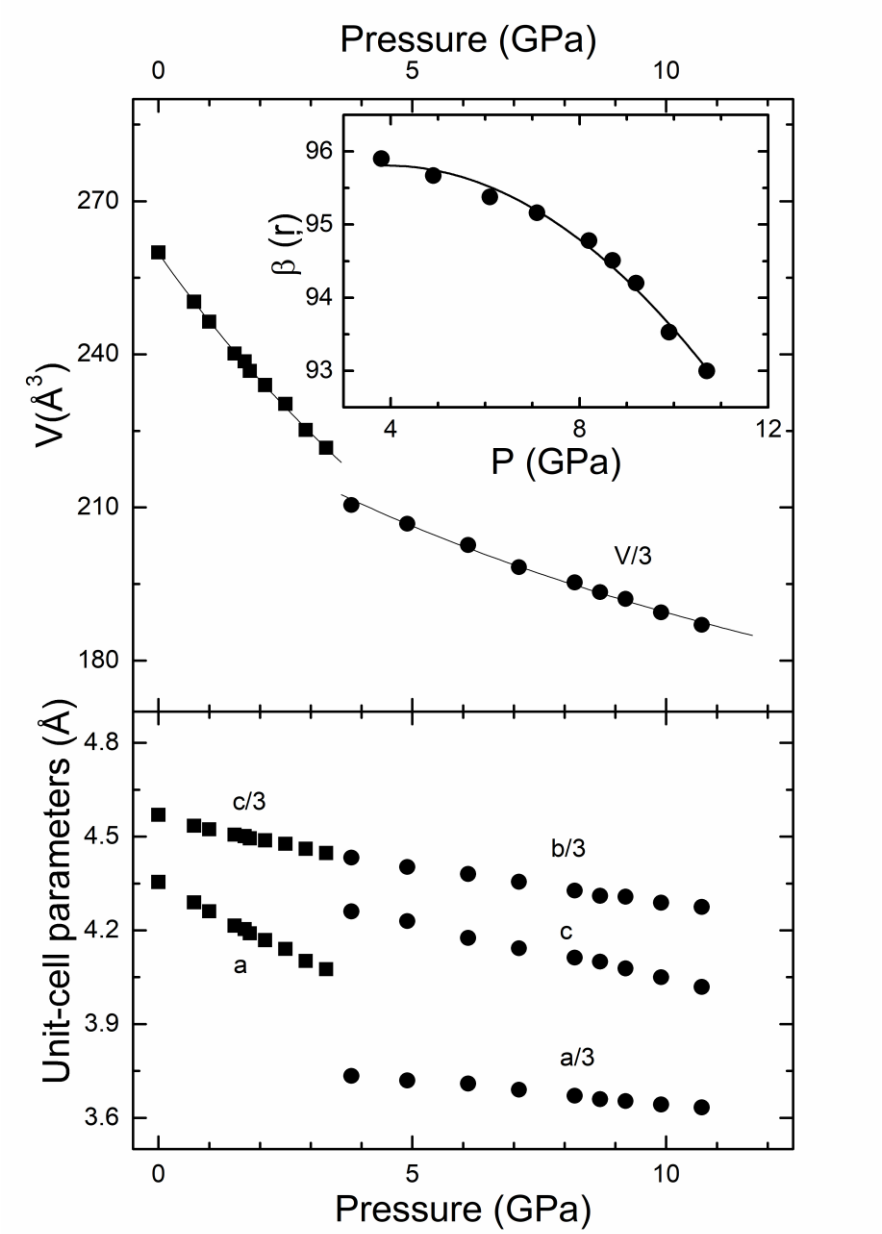

Figure 7. (Top) Pressure dependence of the unit-cell volume for the LP and HP phases of AuI. For the HP phase, we plotted V/3 to facilitate the comparison with the LP phase. Symbols (lines) correspond to experimental (EOS fit) data. The inset shows the pressure dependence of the monoclinic angle in the HP phase. Symbols (line) correspond to experiment (quadratic fit) data. (Bottom) Pressure dependence of the unit-cell parameters for the LP and HP phases of AuI. Some parameters have been divided by 3 for the sake of clarity.

Table 1. Crystal structure of HP phase of AuI at 4.9 GPa (space group P2/m).

a = 11.159(9) Å, b = 13.208(9) Å, c = 4.229(3) Å, β = 95.67(5)°				
	Site	x	y	z
Au_1	4*o*	0.7540(9)	0.1625(9)	0.2704(9)
Au_2	4*o*	0.6225(9)	0.2944(9)	0.8318(9)
Au_3	4*o*	0.8740(9)	0.6678(9)	0.6322(9)
I_1	2*m*	0.6344(9)	0	0.6564(9)
I_2	2*i*	0	0.5867(9)	0
I_3	2*n*	0.7259(9)	0.5	0
I_4	2*n*	0.8276(9)	0.5	0.4909(9)
I_5	2*i*	0	0.2102(9)	0
I_6	2*n*	0.5889(9)	0.5	0.4003(9)

For Table of Contents Only

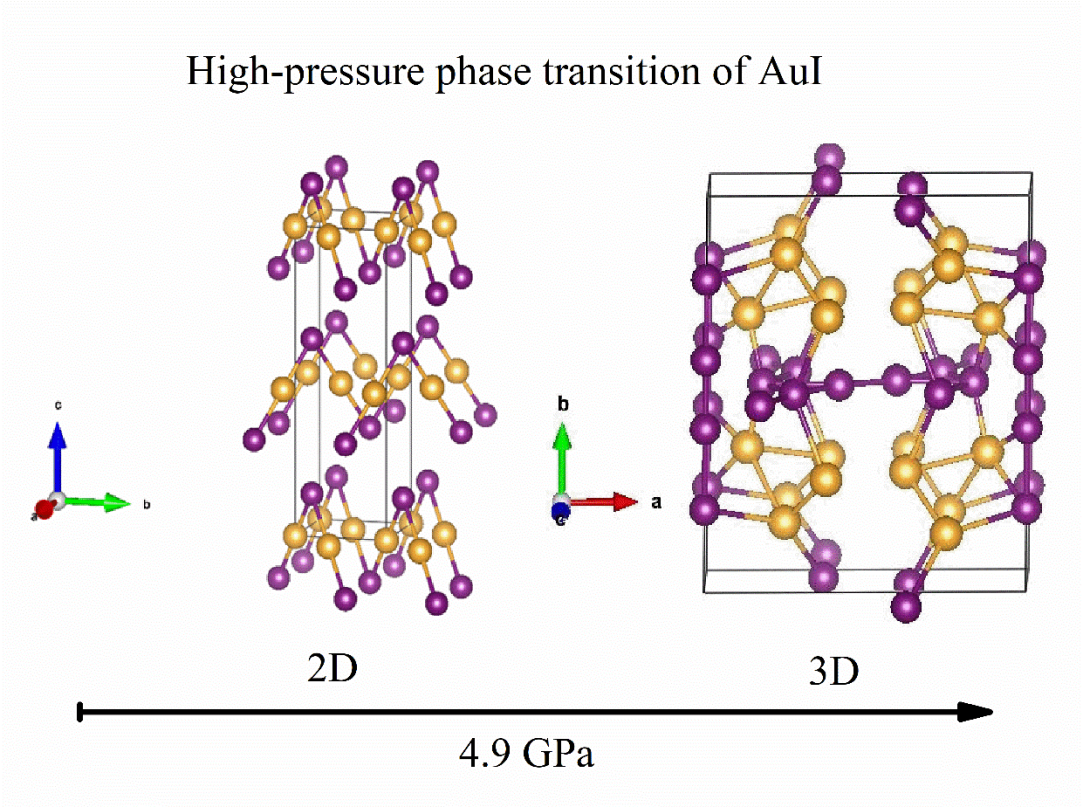

Figure for Table of Contents (TOC): The pressure-induced phase transition of aurophilic AuI has been found at 4.9 GPa. The transformation involves the change from a 2D layered structure, ruled by Au-I covalent, I-I van der waals and Au-Au aurophilic bonds, to a 3D more densely packed structure with Au-I and I-I covalent and Au-Au aurophilic bonds.